Al-Khwarizmi Engineering Journal, Vol. 5, No. 2, PP 20 -31 (2009)

Al-Khwarizmi Engineering Journal

Breast Tumor Diagnosis Using Diode Laser in Near Infrared Region

Munqith S. Dawood* **and** **Ahmed Ali Mohammed****

** Medical Engineering Departmen / College of Engineering / Al-Nahrain University*

*** Biomedical Engineering Department / Al-Khwarizmi College of Engineering / Baghdad University*

ahmed.ali1981@yahoo.com

(Received 11 July 2009; accepted 24 March 2009)

Abstract

In the last years, new non-invasively laser methods were used to detect breast tumors for pre- and postmenopausal females. The methods based on using laser radiation are safer than the other daily used methods for breast tumor detection like X-ray mammography, CT-scanner, and nuclear medicine.

One of these new methods is called FDPM (Frequency Domain Photon Migration). It is based on the modulation of laser beam by variable frequency sinusoidal waves. The modulated laser radiations illuminate the breast tissue and received from opposite side.

In this paper the amplitude and the phase shift of the received signal were calculated according to the original signal for the sake of diagnosis.

These calculations were carried out for different breast thicknesses to find out the best modulation laser beam wavelength and the optimum breast thickness necessary for diagnosis of benign and malignant tumors.

According to our work the most suitable laser wave length to detect the breast tumor for pre- and postmenopausal females was 956 nm and 674 nm for both malignant and benign tumors.

Keywords: *Tumor detection, laser modulation, Photon migration Breast tumor*

1. Introduction

Different methods of breast diagnosis are used; some of these methods are painful like fine needle aspiration or surgical biopsy to examine the slices microscopically to diagnose the tumor (benign or malignant). In the last years a new method was found to detect the breast tumor non-invasively. This method is called Frequency Domain Photon Migration (FDPM) [1]. It is more specific than the other common methods used for breast tumor detection like X-ray mammography, CT scanner, ultrasound, MRI and nuclear medicine. The FDPM is a safe method compared with the other methods because X-ray mammography and CT scanner has some risk of the exposure to their radiation and radioactivities. The MRI is also expensive and cannot detect the micro classification of the breast tissue. The ultrasounds and the other methods cannot differentiate between the benign and the malignant tumor except the nuclear medicine. All these methods used fine needle aspiration or surgical biopsy to differentiate between the benign and malignant.

This new method based on the use of a sinusoidally modulated intensity of diode laser within the NIR (Near Infrared) region to penetrate deeply through the breast tissue which is described as a highly scattering media for light.

A detector in the opposite side of the compressed breast (to reduce the thickness of the breast) is used to collect the laser beam after its penetration through the tissue.

In this paper the FDPM method is discussed and is used to detected and identify the different breast tumors. Theoretically, six laser wavelengths, modulated by different frequencies were used to choose the best one which gives the clearest results.

2. The basic principle of Frequency Domain Photon Migration method

Optical methods applications in medicine are attractive because they are noninvasive, quantitative, and relatively inexpensive and pose no risk of ionizing radiation. The FDPM can successfully be used in vivo to detect the presence of small palpable breast lesions in women with previously diagnosed breast abnormalities [1- 3]. Recently a number of phase resolved optical spectrometers has been developed with the aim of obtaining the absorption coefficient μ_a and the reduced scattering coefficient $\mu_s`$.

Consider that a sinusoidally modulated light source of the form:

$$I = I_0\left(1 + ASin\left(\omega t\right)\right)$$

Passed through the sample of the tissue, where I is the instantaneous detected intensity, I_0 is the peak intensity; A is the modulation depth and ω is the angular modulation frequency. It is clear that a number of parameters can be measured, or calculated after passing the sample of tissue like the phase shift through the sample, and the attenuation of the optical signal as shown in Figure (1).

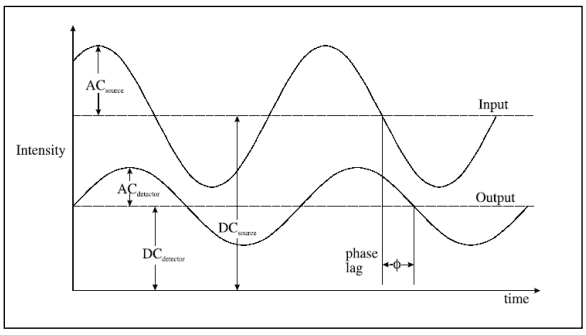

Fig.1. Time Evolution of the Intensity from A Sinusoidally Intensity- Modulated Source.

The detected photon-density wave retains the same modulation frequency as the source photon-density wave but is delayed because of the phase velocity of the wave in the medium. The reduced amplitude of the detected wave arises from attenuation related to the scattering and the absorption processes.

FDPM employs intensity-modulated NIR light to characterize tissue quantitatively in terms of its optical parameters; i.e., the reduced-scattering coefficient (μ_s') and the absorption coefficient (μ_a). The concentration of significant NIR absorbers like deoxyhemoglobin (Hb), oxyhemoglobin (HbO_2), water, and adipose can be calculated by using the measured μ_a values [2, 5]. Multiple scattering of light in breast tissue occurs as a consequence of spatial variations in refractive index, which are influenced by cellular and extracellular matrix density [6]. Both μ_a and μ_s' provide an understanding of changes in tissue cellularity, metabolic activity, physiology, and host response to cancer. Detection of lesions is based on the functional contrast between normal and diseased tissue in the same patient. However, the physiology of healthy breast tissue is complex, influenced by multiple internal and external factors such as menstrual-cycle phase, menopausal status, exogenous hormones, lactation, and pregnancy. Consequently, to establish a better basis for optical detection and diagnosis based on differential functional contrast, the optical properties of normal breast tissue must be carefully examined and characterized.

This technique can be useful for the detection of the physiological status and changes in biological tissues. Therefore, great effort has already been expended in developing noninvasive optical methods for early diagnosis of breast cancer. These methods are based on the detection of changes in optical characteristics, like the absorption and scattering coefficients, μ_a and μ_s' of the normal and malignant tissues. The optical methods have their problems arise from the fact that natural variations in the absorption and scattering in normal tissues of different patients exceed the changes in the parameters due to pathological modification of a tissue from an individual. This dictates the necessity for comparison of μ_a and μ_s' in the normal and pathologically modified tissues of individual patients. The Beer–Lambert law in its simple form is not valid for turbid media because photons pass through a scattering medium along trajectories of various lengths and forms [7].

In this paper the breast optical properties of healthy and tumor tissues were used in a FDPM mathematical model of breast tissue for different wavelengths (674, 782, 803, 849, 894, 956 nm) and different thicknesses of breast tissue ranging from 0.5 cm to 7.5 cm of premenopausal and postmenopausal females. A number of curves are drawn of the detected amplitude and phase shift of the simulated received laser intensity versus the frequency of the modulated AC signal that ranged up to 1GHz for each wavelength.

3. Laser Interaction with Biological Tissue

To study the tissue optical properties, we must understand the laser interaction with tissue, which is summarized in five forms as shown in figure (2): reflection, refraction, absorption, scattering and transmission. Two other factors must be considered also, which are tissue factors and clinical factors. The tissue factors include the contents of tissue like the water, lipid, blood, organism, tissue thickness, tissue layers and types of tissues. While the clinical factors include laser power, laser beam, laser intensity and the stile of laser delivery (pulse or continuous) and the angle of beam incidence as well as the duration of exposure.

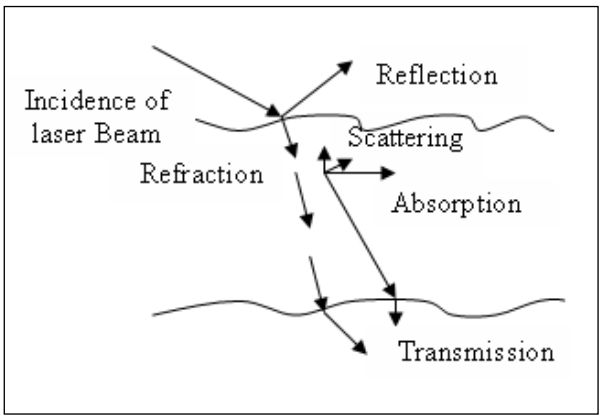

Fig.2. The Types of Laser Energy Interaction with Tissue.

4. Laser Propagation in Biological Tissue

These optical tissue properties essentially depend on the wavelength of the incident laser, the index of refraction, the attenuation and scattering coefficients μ_a and μ_s of the tissue.

In the visible electromagnetic spectrum, the most important absorbers of biological tissue are melanin in the skin and hemoglobin in the blood; whereas in the near and mid infrared, water absorption becomes dominant. The scattering continuously decreases from UV towards the infrared [8].

Human tissues contain a variety of substances whose absorption spectra at NIR wavelengths is well defined, and which are present in sufficient quantities to contribute significant attenuation to the transmitted light. The concentration of some absorbers, such as water, melanin, and bilirubin, remains virtually constant with time. However, some absorbing compounds, such as oxygenated hemoglobin (HbO_2), deoxyhaemoglobin (Hb), and oxidized cytochrome oxidaze (CtOx) have concentrations in tissue, which are strongly linked to tissue oxygenation and metabolism. Increasingly dominant absorption by water at longer wavelengths limits spectroscopic studies to less than about 1000 nm. The lower limit on wavelength is dictated by the overwhelming absorption of Hb below 650 nm. However, within the 650-1000 nm window, it is possible with sensitive instrumentation to detect laser, which has traversed up to 8 cm of tissue [9].

5. Breast Tissue

One of the major structural features of breast tissue is the large adipose fraction typically near the periphery of the breast, as shown in Figure (3), which is thought to be an average of nearly 75% in women. However, a large variation exists among individuals, based on body mass index and breast size [10]. In the interior of the breast, there is often glandular tissue, which has higher blood content and hence higher water content. This area is thought to have a higher scattering power, perhaps owing to smaller scattering sites. Although the origin of the scattering has not been established clearly in areas of adipose tissues where fat content is high, the scattering power is low, again perhaps because of the larger scattering centers of the lipid-filled cellular space. The scattering power is high in the interior of the breast and decreases toward the exterior [11]. The breast tissue is surrounded by a layer of skin that covers it from all directions that lead to extra scattering media for penetrating light.

The breast is a gland designed to make milk. The lobules in the breast make the milk, which then drains through the ducts to the nipple as shown in Figure (3). Like all parts of the body, the cells in the breasts usually grow and then rest in cycles. The periods of growth and rest in each cell are controlled by genes in the cell's nucleus. The nucleus is like the control room of each cell. When the genes are in good working order, they keep cell growth under control. However, when the genes develop an abnormality, they sometimes lose their ability to control the cycle of cell growth and rest.

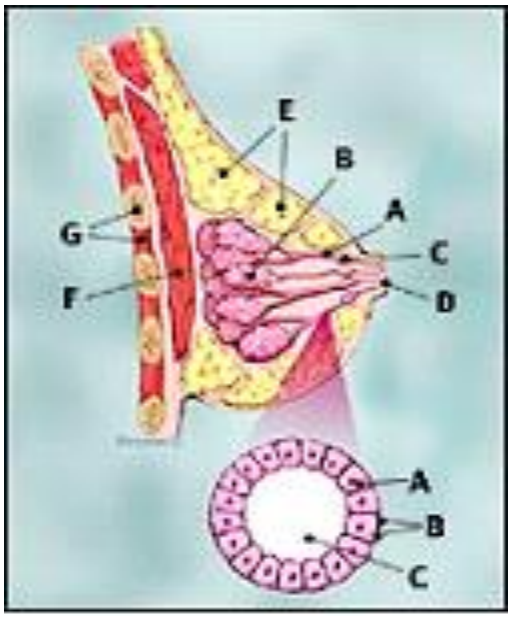

Fig. 3. The Histology of the Breast Tissue Where the Breast Profile Is:- 1-Breast profile: A=Ducts, B=Lobules, C=Dilated section of duct to hold milk, D=Nipple, E=Fat, F=Pectoralis major muscle, G=Chest wall/ribcage, 2- Enlargement: A=Normal duct cells, B=Basement membrane, C=Lumen (center of duct).

6. Breast Cancer

Cancer occurs when cells become abnormal and keep dividing and forming more cells without control or order. This creation of mass of extra tissue, called a growth or tumor, can be benign or malignant. The presence of these cancerous tumors within the healthy breast tissue will change its optical parameters.

In this paper, we study the effect of these changes in optical parameter of breast tissue due to the presence of ductal carcinoma in situ (DCIS), Invasive Ductal Carcinoma (IDC), Invasive Lobular Carcinoma (ILC) and Fibroadinoma.

7. Frequency Domain

Since any measurement in the time domain can be equivalently expressed in the frequency domain, techniques have also been developed which have sought to acquire transmitted light information in the frequency domain directly. The frequency domain techniques involve illuminating the object tissue with an intensity-modulation beam, and measuring its amplitude and phase shift after passing through the tissue. The transport of the modulated beam is often described in terms of the propagation of so-called photon density waves.

Most experimental work performed so far has utilized frequencies of a hundred MHz, which are equivalent to a temporal resolution of a few nanoseconds and photon density wavelengths of the order of a nanometer [8]. Frequency domain techniques allow for the separation of the absorbing properties from the scattering properties of multiple-scattering media [12].

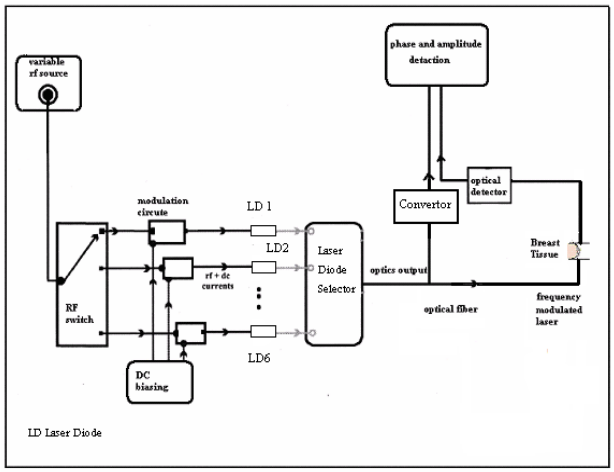

Fig. 4. Schematic Diagram Representing the Application of FDPM Method in Breast Cancer Diagnosis.

8. Frequency Domain Photon Migration System

An overall view of the frequency domain photon migration (FDPM) instrument is schematically depicted in Figure (4). The FDPM instrument is constructed to measure phase and amplitude of photon density waves over a broad range of modulation frequencies and for different optical wavelengths. Measurements of phase and amplitude over the range of modulation frequencies are performed in a sequential fashion for each wavelength. Selection of a specific wavelength is achieved through coordinated switching of different RF to modulate different diode laser circuits.

A DC current source provides constant biasing current to each diode. The basic circuit superimposes the RF signals with the DC currents; the combined currents are used to derive a given laser. Thus, the diode will produce a sinusoidal modulated lasers. The DC bias and RF modulation currents are uniquely set for each

diode laser by considering their maximum current ratings and RF impedance characteristics.

Presently, six diode lasers at 674, 782, 803, 849, 894 and 956 nm are used; however, additional diode lasers can be readily incorporated to extend the wavelength spectrum of the FDPM instrument.

The optical switch couples intensity-modulated light to a selected output port. RF and optical switching are coordinated so that only one diode laser is modulated at a time. The phase data represent the phase difference between the sample and reference signal, while the amplitude data represent a ratio between the sample and reference signal amplitude of the normal tissue.

9. The Theory

Light propagation in tissue can be modeled as transport of particles, which perform a random (walk) in the scattering medium due to multiple collisions. Thus, the photon diffusion approach is an appropriate way of describing light propagation in a highly scattering media. The diffusion equation is a useful approximation of Boltzmann transport equation. It describes well the light transportation in a multiple scattering media of thickness d [2, 5, and 12]:

$$-D(d)\nabla^2\phi(d,t)+\mu_a(d)\phi(d,t)=S_0(d) \quad \ldots(1)$$

where d is the source detector distance, μ_a is the absorption coefficient, $S_0(d)$ is the photon source term and *D(d)* is the diffusion coefficient. The diffusion approximation can be used in the case of the mean free path for light absorption more than the mean free path for light scattering.

In tissues, light scattering is primarily in the forward direction at a microscopic level, but on the length scale of the reduced scattering coefficient, the photon flux is isotropic.

The photon flux, Φ (d, t), (photons.cm^{-2}.s^{-1}) that moves along a photon density gradient, U (d, t), (photons.cm^{-3}) is [2]:

$$\phi(d,t)=-\frac{\nu}{3(\mu_a+\mu_s')}\nabla U(d,t)=-\nu D\nabla U(d,t) \quad \ldots(2)$$

where ν represents the photon frequency, and D represents the diffusion coefficient given by:

$$D=1/3(\mu_a+\mu_s') \quad \ldots(3)$$

where μ_s' is the reduced scattering coefficient and it is represented by :

$$\mu_s'=\mu_s(1-g).$$

where g is the average of the cosine of the scattering angle.

The source term is usually considered an isotropic emitter located at the origin
in the frequency-domain. The intensity of the light source is modulated at a frequency (ω/2π), and the photon density wave is:

$$U=DC+AC\exp[-i(\omega.t-\Phi)] \quad \ldots(4)$$

where AC represents the amplitude (alternate component), DC is the time-averaged intensity (direct component), and Φ is the phase of the photon density wave.

In the frequency-domain spectroscopy, considering a homogeneous medium, the source term is a spherical photon density wave:

$$S_0(d,t)=S.\delta(d).[1+A\exp(-i\omega.t)],$$

where δ (d) is the Dirac function at the source-detector distance *d*, *S* is the source strength (in photons.s^{-1}), and A is the modulation depth of the source.

The absorption coefficient μ_a is the inverse mean distance a photon travels before it is absorbed. The absorption coefficient has units of reciprocal distance, and is typically 0.05–0.3 cm^{-1} for tissues in the wavelength region between 700 nm and 900 nm [13]. The reduced scattering coefficient μ_s' is a measure of scattering per unit distance, and is typically 4 – 15 cm^{-1} for tissues. The reduced scattering coefficient refers to effectively isotropic scattering events and it is given by the inverse of the mean distance over which a photon loses the memory of its original direction of propagation. In tissues, the μ_s' is typically one order of magnitude bigger than μ_s.

For an infinite, macroscopically uniform medium, the diffusion equation of a sinusoidal intensity-modulated point source for the photon density U(d, t) at a distance d relative to the source at time t to yield (in photons per unit volume) could be presented as follows [12]:

$$U(d,t)=\frac{S}{4\pi \mathbf{v}Dd}\exp\left[-d\left(\frac{\mu_a}{D}\right)^{1/2}\right]+\frac{SA}{4\pi \mathbf{v}Dd}$$
$$\exp\left\{-d\left(\frac{\mathbf{v}^2\mu_a^2+\omega^2}{\mathbf{v}^2D^2}\right)^{1/4}\cos\left[\frac{1}{2}\tan^{-1}\left(\frac{\omega}{\mathbf{v}\mu_a}\right)\right]\right\}$$
$$\times\exp\left\{id\left(\frac{^2\mu_a^2+\omega^2}{\mathbf{v}^2D^2}\right)^{1/4}\cdot\right.$$
$$\left.\times\sin\left[\frac{1}{2}\tan^{-1}\left(\frac{\omega}{\mathbf{v}\mu_a}\right)\right]-i(\omega t-\varepsilon)\right\} \quad \ldots(5)$$

The speed of each photon in the medium surrounding the scattering particles is given by v = $(3.00\times10^{10}$cm/s)/n, n being the index of refraction of the transporting medium, where $\mu_s`$ is the reduced scattering coefficient, and μ_s is the scattering coefficient. *S* is the source strength (in photons per second), A is the modulation depth of the source, and ε is the phase of the source. In Eq. (5), it is predicted that the photon density U(d, t) is generated by an isotropically emitting, sinusoidally intensity-modulated point source immersed in an infinite medium which constitutes a scalar field that propagates at a constant speed in a spherical wave and attenuates as a decaying exponential in d, divided by d, as it propagates.

The photons injected into the medium are initially scattered at a distance of $1/(\mu_a+\mu_s`)$ (i.e., one mean free path) from the end of the optical fiber source [14]. The assumption is that these first interactions are sufficiently localized that a simple Diracdelta function accurately describes the light propagation when $d>>1/\mu_s$.

The source terms S, A, and ε are obviously independent of the quantities of interest, namely, the absorption and scattering coefficients $[\mu_a(\lambda),\mu_s`(\lambda)]$ of the medium at some light wavelength λ. Ideally the source terms are also independent of ν, but in practice they are not. One possibility that eliminates these source terms from a measurement at a given ν is to measure the properties of the photon density at two different source/detector separations, namely, d and d_0, and compare the quantities obtained at these two distances. Eq. (5) yields expressions for quantities obtained at d relative to the corresponding quantities obtained at d_0, namely, the steady-state photon density DC, the amplitude of the photon-density oscillations AC, and the phase shift of the photon-density wave φ. The relative quantities are given by [15]

$$DC_{rel}=\frac{DC(d)}{DC(d_0)}=\frac{d_0}{d}\exp\left[-(d-d_0)\left(\frac{\mu_a}{D}\right)^{1/2}\right], \quad \ldots(6)$$

$$AC_{rel}\equiv\frac{AC(d)}{AC(d_0)}=\frac{d_0}{d}\exp\left\{-(d-d_0)\left(\frac{\mathbf{v}^2\mu_a^2+\omega^2}{\mathbf{v}^2D^2}\right)^{1/4}\times\cos\left[\frac{1}{2}\tan^{-1}\left(\frac{\omega}{\mathbf{v}\mu_a}\right)\right]\right\} \quad \ldots(7)$$

$$\varphi_{rel\equiv}\varphi(d)-\varphi(d_0)=(d-d_0)\left(\frac{\mathbf{v}^2\mu_a^2+\omega^2}{\mathbf{v}^2D^2}\right)^{1/4}\times\sin\left[\frac{1}{2}\tan^{-1}\left(\frac{\omega}{\mathbf{v}\mu_a}\right)\right]. \quad \ldots(8)$$

The relative demodulation of the photon-density wave is given by

$$M_{rel\equiv}\,AC_{rel}/DC_{rel} \quad \ldots(9)$$

Our frequency-domain data are obtained in a manner that allows for fitting these data (i.e., DC_{rel}, AC_{rel}, φ_{rel}, and M_{rel}) directly to Eqs. (6)– (9) to obtain the absorption and the reduced scattering coefficients $[\mu_a(\lambda),\mu_s`(\lambda)]$ of the multiple-scattering medium at some light wavelength λ. Note that in the three equations [Eqs. (6)– (8)], there are only two unknowns, namely, $\nu\mu_a$ and vD, where D is given by Eq. (3). We assume that the index of the refraction of the transporting medium is known, so that explicit values for $\mu_a(\lambda)$ and $\mu_s`(\lambda)$ can be recovered from the quantities $\nu\mu_a$ and vD. This means that in principle only two out of the three expressions in Eqs. (6) – (8) are needed to determine $\mu_a(\lambda)$ and $\mu_s`(\lambda)$ at a single modulation frequency $\omega/2\pi$, using different combinations of Eqs. (6) – (8).

10. Results

In our work on the theoretical simulation, the results of calculations are presented in thirty two figures to compare the effect of using six laser wavelengths (674, 782, 803, 849, 894, and 956 nm): sixteen figures for premenopausal female and sixteen for female. The figures show the calculated variations of the amplitude and phase shift of the received laser light based on FDPM method. The results in each figure are presented by four curves: one for normal breast tissue and three for different breast tumors (DCIS, Fibroadinoma and Invasive Carcinoma). The calculations were carried out for modulation frequencies ranged up to 1 GHz for different breast thicknesses.

In this paper we present only four groups of the curves in figures 5 a, b, 6 a, b, 7 a, b, and 8 a, b.

Figures (5 and 6) are for premenopausal female and figure (7 and 8) are for postmenopausal female. The figures for amplitude and phase shift versus RF frequency modulation are shown for different tissue thickness, and different wavelength (λ = 674, 782, 803, 849, 894, and 956 nm); the aim is finding out the best wavelength to be used in cancer diagnosis and for different female ages.

Figures (5 and 7) are carried out and for 0.5 cm tissue thickness and figure (6 and 8) are carried out for 5.5 cm tissue thickness.

11. Discussion

Pre- and postmenopausal normal breasts exhibit clear wavelength-dependent differences in both absorption and scattering parameters. The scattering is approximately 20% greater in pre-menopausal (μ_s' ~ 0.8 to 1.1 mm^{-1}) group of women than in post-menopausal women (μ_s' ~ 0.67 to 0.86 mm^{-1}). In addition, the wavelength dependence of scattering is steeper for premenopausal women. These findings are consistent with known changes in breast physiology. Breast tissue, while under hormonal control, has higher glandular/cellular content and collagen is required in the extracellular matrix in order to support the structural demands of cellular proliferation. After menopause, the absence of hormonal stimulation results in glandular shrinkage, collagen remodeling to fat and diminished vasculature. Since small tissue structures such as collagen fibers and subcellular organelles are likely to be the primary contributors to tissue scattering, it is not surprising that the wavelength dependence of scattering is relatively steep for premenopausal women. In contrast, following conversion to a principally large-particle fatty matrix, a much more gradual wavelength dependence of scattering is observed. Thus, the diminished contribution of the glands and collagenous stroma leads to a clear wavelength-dependent scattering reduction. Variations in absorption can be explained in a similar manner.

These results demonstrate the intrinsic sensitivity of FDPM to breast tissue physiological states. In order to address the origin of photon migration signals in solid tumors, we have initiated breast tumor studies in human subjects. From the resulting curves in Figures (5, 6, 7, and 8), there are two-fold advantages: 1) enhanced early detection of relatively small lesion even with long distance between the source and the detector (0.5 to 7.5 cm thickness, and 2) more specific characterization of benign versus malignant lesions would lead to reductions in the large but unnecessary surgical biopsies.

The method FDPM is useful to differentiate between the types of tumors and the normal tissues.

According to the figures used in multi thicknesses between 0.5 – 7.5 cm and multi frequency modulation from 0 – 1GHz, the curves clearly differentiate between the tumors and health tissue as shown in figures (5 – 8), for the wavelengths 674 nm and 956 nm, in the amplitude. Because the tumors are close to each other and to the normal curve, the Fibroadinoma and the Invasive carcinoma are very clear to be differentiate but the Invasive carcinoma in situ is not very clear differentiated because it is closed to the normal curve so it must be diagnosed by two wavelengths (674 and 956 nm). The best modulation frequencies that we can diagnose the tumors very clearly thoroughly rang between 800 MHz to 1 GHz. So to get the best result for beast tumor diagnoses, we suggest using two wave lengths 674 nm and 956 nm at both amplitude and phase shift and at frequency modulation between 800 MHz to 1GHz to avoid the mistake. For postmenopausal female, the recommended thicknesses are between 0.5 to 5.5 cm.

Average premenopausal μ_a values (0.0048–0.015 mm^{-1}) at each wavelength are 2.3-to 3-fold higher than postmenopausal absorption (average μ_a = 0.0016–0.0064 mm^{-1}). Furthermore, all postmenopausal μ_a values are less than 0.007 mm^{-1}. Premenopausal women have 16 –22% higher

scattering values at each wavelength (average μ_s` = 0.83-1.1 $mm^{-1}$) than postmenopausal subjects (average $\mu_s$` = 0.67– 0.86 mm^{-1}) [9].

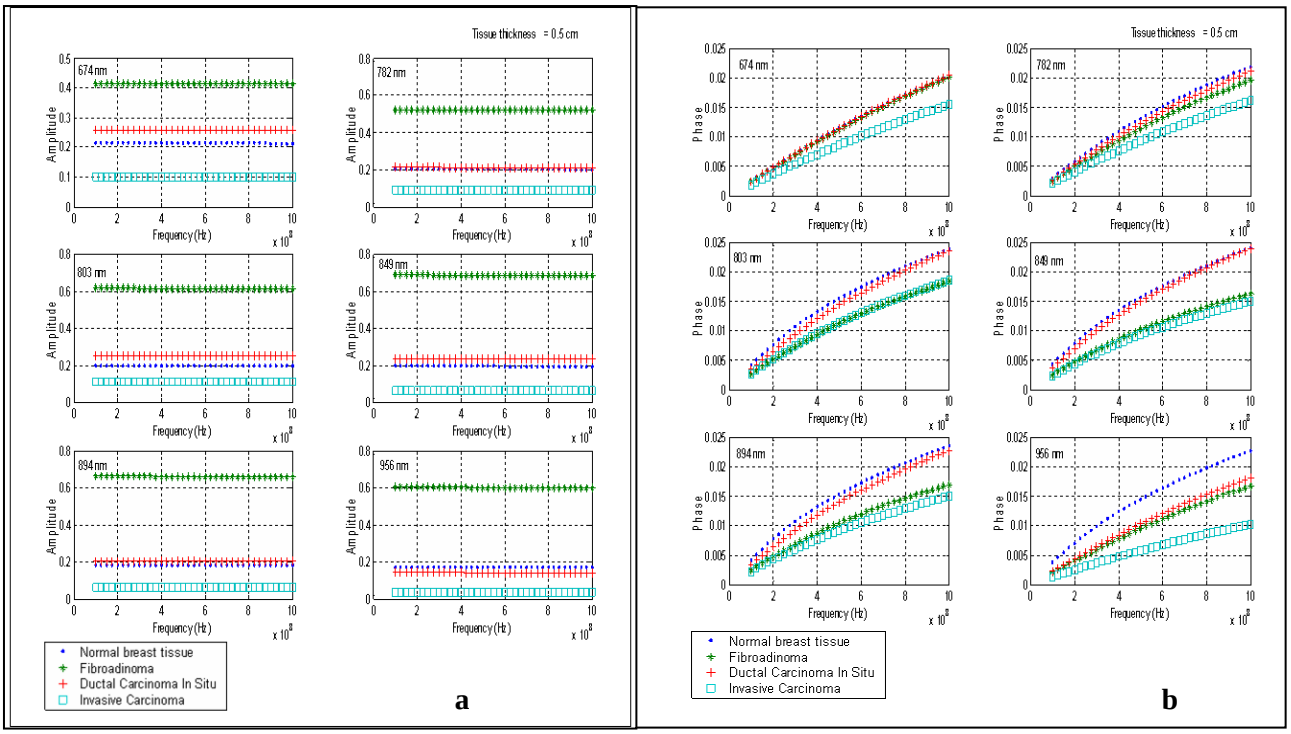

Fig.5. a) The Amplitude (AC) of the Detected Laser Signal vs. The Modulation Frequency, b) The Phase Shift φ of the Detected Signal vs. the Frequency for Laser Wavelength (λ = 674, 782, 803, 849, 894, and 956 nm) at Tissue Thickness 0.5 cm for Premenopausal Female.

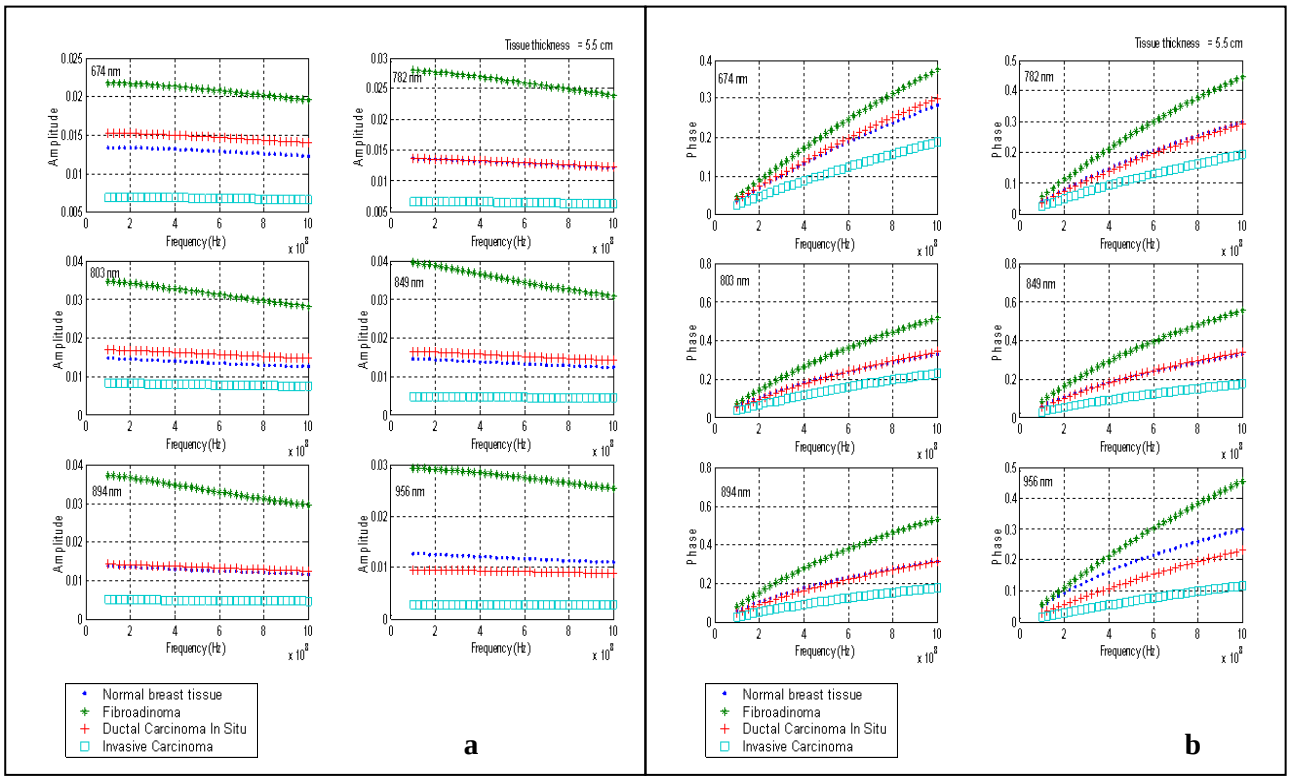

Fig. 6. a) The Amplitude (AC) of the Detected Laser Signal vs. The Modulation Frequency, b) The Phase Shift φ of the Detected Signal vs. The Frequency for Laser Wavelength (λ = 674, 782, 803, 849, 894, and 956 nm) at Tissue Thickness 5.5 cm for Pretmenopausal Female.

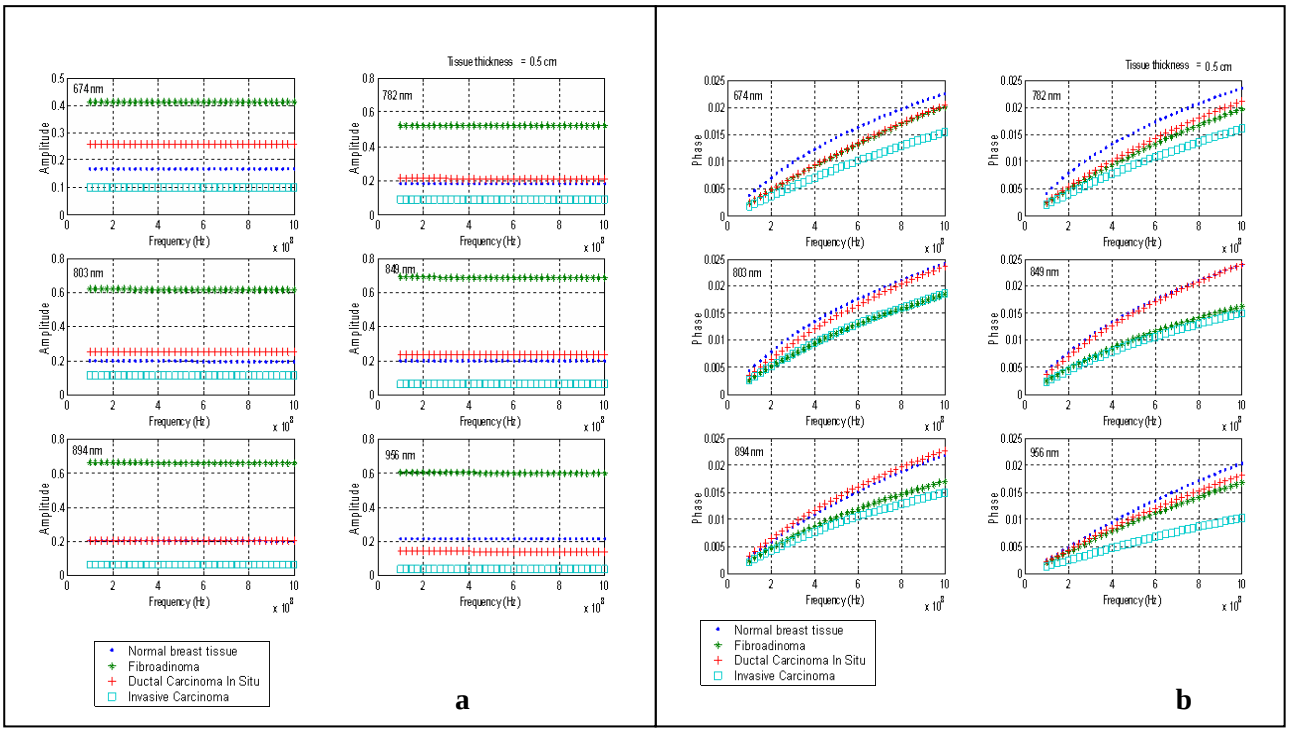

Fig. 7. a) The Amplitude (AC) of the Detected Laser Signal vs. The Modulation Frequency, b) The Phase Shift φ of the Detected Signal vs. The Frequency for Laser Wavelength (λ = 674, 782, 803, 849, 894, and 956 nm) at Tissue Thickness 0.5 cm for Postmenopausal Female.

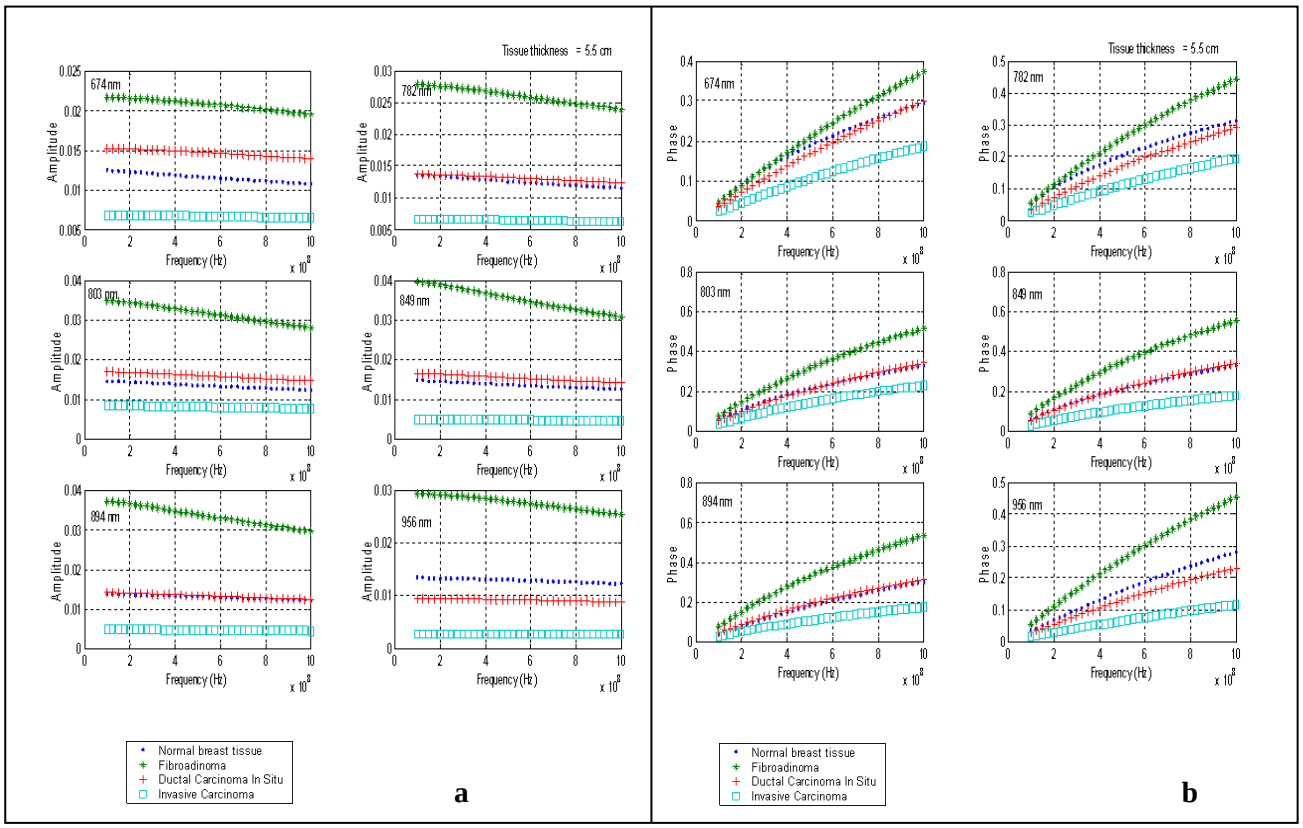

Fig. 8. a) The Amplitude (AC) of the Detected Laser Signal vs. The Modulation Frequency, b) The Phase Shift φ of the Detected Signal vs. The Frequency for Laser Wavelength (λ = 674, 782, 803, 849, 894, and 956 nm) at Tissue Thickness 5.5 cm for Postmenopausal Female.

The coefficient of scattering changes versus wavelength for post- and premnopausal are shown in figure 9.

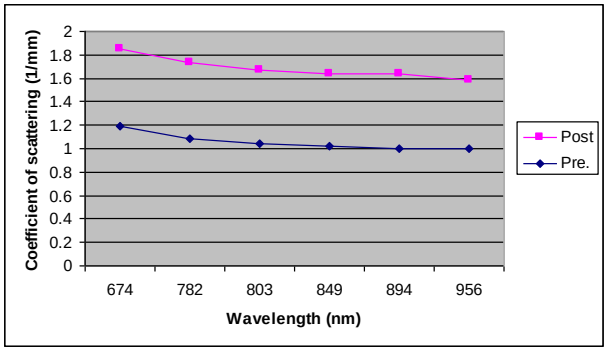

Fig. 9. Coefficient of Scattering vs. Wavelength for Pre. and Postmenopausal Females.

The gradual $\mu_s`$ vs. $\lambda$ slope shown in Figure (9) for the postmenopausal subjects reflects large particle scattering consistent with a high percentage of fatty parenchyma found in this age group. In younger women, the relatively steep $\mu_s`$ vs. λ slope is likely to be influenced by the presence of extracellular collagen in addition to cellular/epithelial factors

Physiological differences between tumor and normal tissue are further amplified by calculations of water and blood content. [3].

The tumor absorption is consistent in the order of 2- to 3.5-fold greater than normal tissue, as shown in Figure (10) because in the regions of tumor the blood supply vessels are accumulated more widely than in the normal tissue.

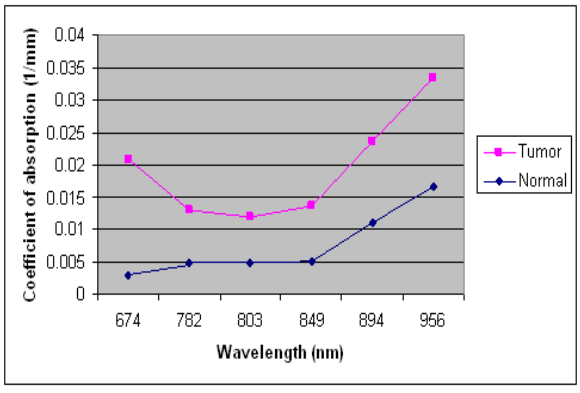

Fig.10. Coefficient of Absorption of Normal and Tumor Breast Tissues vs. Wavelength.

12. Conclusions

From the previous result, the best wavelengths used in this method are 674 and 956 nm.

The best results in this work appear very clear in the frequency modulation ranging from (800 MHz to 1000 MHz).

At small thicknesses of breast tissue, approximately between 0.5 to 2.5 cm, the tumor is difficult to be differentiated clearly in the wavelength 956 nm due to the insufficient absorption and scattering. So the received spectral amplitude and phase shift are very clear at breast tissue thicknesses that exceed 2.5 cm at 956 nm for modulation frequencies ranging from 800 MHz to 1000 MHz.

13. References

[1] Payam Heydari, Pai Chou, Keun Sik No,"High Frequency, Miniaturized FDPM Integrated System-On-A-Chip",NTROI Retreat Poster List, 2004.

[2] Lelia Adelina Paunescu." Tissue Blood Flow and Oxygen Consumption Measured with Near-Infrared Frequency-Domain Spectroscopy", Ph.D. thesis Graduate College, the University of Illinois at Urbana-Champaign, 2001.

[3] S. Fantini, S. A. Walker, M. A. Franceschini, M. Kaschke, P. M. Schlag, and K. T. Moesta, ''Assessment of the size, position, and optical properties of breast tumor in vivo by noninvasive optical methods,'' Appl. Opt. 37, 1982–1989 (1998).

[4] Tromberg, B. J., Coquoz, O., Fishkin, J. B., Pham, T., Anderson, E. R., Butler, J., Cahn, M., Gross, J. D., Venugopalan, V. & Pham, D." Non-invasive measurements of breast tissue optical properties using frequency-domain photon migration" hilos. Trans. R. Soc. London, B 352, 661–668. 1997.

[5] Ryan Lanning, Bruce Tuomberg. "Non-Invasive Characterization of Breast Cancer Using Near Infrared Optical Spectroscopy". The UCI Undergraduate Research Journal 2000, pp. 43-50.

[6] Tuan H. Pham, Olivier Coquoz, Joshua B. Fishkin, Eric Anderson, and Bruce J. Tromberg. "Broad Bandwidth Frequency Domain Instrument for Quantitative Tissue Optical Spectroscopy". Review of Scientific Instruments, Vol. 71, No. 6, June 2000.

[7] Vladimir Liger, Alexander Zybin, Mikhail Bolshov, and Kay Niemax."Dual Wavelength Method for Molecular Difference Absorption Measurements in Turbid Media". Applied Spectroscopy Vol.56, No. 2, 2002, pp. 250-256.

[8] J. B. Fishkin, E. Gratton, M. J. vandeVen, and W. W. Mantulin, ''Diffusion of intensity-modulated near-Infrared light in turbid media,'' in Time-Resolved Spectroscopy and Imaging of Tissues, B. Chance and A. Katzir, eds., Proc. Soc. Photo-Opt. Instrum. Eng. 1431, 122–135, 1991.

[9] Clare Elwell and Hebden Jem."Near-Infrared Spectroscopy". UCL, Biomedical Optical Research Laboratory, January 6, 1999.

[10] Grazia Arpino1, Valerie J Bardou 2, Gary M Clark1 and Richard M Elledge. "Infiltrating Lobular Carcinoma of the Breast: Tumor Characteristics and Clinical Outcome". Breast Cancer Research, Vol 6, No 3, 2004.

[11] Breast Net http://www.bci.org.au "Ductal Carcinoma in situ (DCIS), "An information guide for patients. NSW Breast Cancer Institute, 2004.

[12] Joshua B. Fishkin, Peter T. C. So, Albert E. Cerussi, Sergio Fantini,Maria Angela Franceschini, and Enrico Gratton." Frequency-domain method for measuring spectral properties in multiple-scattering media: methemoglobin absorption spectrum in a tissue like phantom". Applied Optics, Vol. 34, No. 7, 1 March 1995.

[13] D. Levitz, L. Thrane, M.H. Frosz, P. E. Andersen, C. B. Andersen, J. Valanciunaite, J. Swartling, S. Andersson-Engels, and P. R. Hansen. "Determination of Optical Scattering Properties in Highly-Scattering Media in Optical Coherence Tomography Images". Opt. Expr. 12, 249-259 (2004).

[14] D. M. Hueber1, M A Franceschini, H Y Ma, Q Zhang J R Ballesteros, S Fantini, D Wallace, V Ntziachristos and B Chance." Non-invasive and quantitative near-infrared haemoglobin spectrometry in the piglet brain during hypoxic stress, using a frequency-domain multidistance instrument" Phys. Med. Biol. 46 (2001) 41–62. www.iop.org/Journals/pb.

[15] Patterson M. S., Chance B, and Wilson B. C., ''Time Resolved Reflectance and Transmittance for the Noninvasive Measurement of Tissue Optical Properties,'' Applied. Optics. 28, 2331–2336, (1989).

تشخيص اورام الثدي باستخدام ليزرالدايود

منقذ سليم داود* و احمد علي محمد**
*قسم الهندسة الطبية/ كلية الهندسة/ جامعة النهرين
** قسم الهندسة الطب الحياتي/ كلية الهندسة الخوارزمي/ جامعة بغداد
ahmed.ali1981@yahoo.com

الخلاصة

استخدمت في السَنَوات الاخيرة طريقة حديثة لتشخيص اورام الثدي باستخدام الليزر وبدون تدخل جراحي للاناث قبل وبعد سن اليأس. استندت هذه الطرائق على إستعمال إشعاعِ الليزرِ وهي الأكثر أماناً مِنْ بين الطرائق المستعملةِ في يومنا هذا لكشفِ اورم الثدي , مثل تصوير الثدي اشعاعيا باستخدام الاشعة السينيةِ، كما في جهاز المفراس الحلزوني،و الاشعة النووية كما في اجهزة الطب نووي.

تدعى إحدى هذه الطرائقِ الجديدةِ إف دي بي إم (هجرة الفوتونِات بمجالِ ترددي). تستند هذه الطريقة على تحويرِ شعاعِ الليزرِ للموجات الجيبية بترددات متغيّرةِ. تدخل إشعةُ الليزرِ المُنَظَّمةِ نسيجِ الثدي وتستلم مِنْ الجانبِ المعاكسِ.

لقد تم قياس ارتفاع و تقدم او تأخر الموجة النافذة مقارنة بالموجة الاصلية لاجل التشخيص.

هذه الحساباتِ حُمِلتْ لقياسات سُمكيَة مُختلِفة للثدي لإكتِشاف أفضل طولِ موجي لاشعاعِ اليزرِ و افضلِ سُمكِ ضروريِ للثدي لتشخيصِ الأورامِ الحميدةِ والخبيثةِ فيه.

ان طول موجةِ الليزرِ الأكثر ملائمة لإكتِشاف اورامِ الثدي للإناث قبل وبعد سن اليأس كَانَ 956 نانوميتر و674 نانوميتر لكلتا الأورام الخبيثة والحميدة.